Electronic Supplementary Information

Developing an Abnormal high-Na-Content P2-Type Layered Oxide Cathode with Near-Zero-Strain for High-Performance Sodium-Ion Battery

Hai-Yan Hu,‡[ab] Jia-Yang Li,‡[b] Yi-Feng Liu,[b] Yan-Fang Zhu,*[ab] Hong-Wei Li,[b] Xin-Bei Jia,[ab] Zhuang-Chun Jian,[ab] Han-Xiao Liu,[ab] Ling-Yi Kong,[ab] Zhi-Qi Li,[ab] Hang-Hang Dong,[b] Meng-Ke Zhang,[d] Lang Qiu,[d] Jing-Qiang Wang,[b] Shuang-Qiang Chen,[ab] Xiong-Wei Wu,[c] Xiao-Dong Guo[d] and Yao Xiao*[ab]

[a] Institute for Carbon Neutralization, College of Chemistry and Materials Engineering, Wenzhou University, Wenzhou, 325035, P.R. China.

Email: yanfangzhu@wzu.edu.cn; xiaoyao@wzu.edu.cn;

[b] Wenzhou Key Laboratory of Sodium-Ion Batteries, Wenzhou University Technology Innovation Institute for Carbon Neutralization, Wenzhou, 325035, P.R. China.

[c] School of Chemistry and Materials Science, Hunan Agricultural University, Changsha, 410128, P.R. China.

[d] College of Chemical Engineering, Sichuan University, Chengdu, 610065, P.R. China.

‡ These authors contributed equally to this work.

Experimental section

Material synthesis. The resulting cathode materials, $NaNi_{1/3}Co_{1/3}Mn_{1/3}O_2$ (NaNCM) and $NaNi_{2/9}Mg_{1/9}Co_{1/3}Mn_{1/3}O_2$ (NaNMCM) were prepared *via* thermal polymerization combined with high temperature calcination. The stoichiometric mounts of $C_2H_3O_2Na$ (99.99%), $C_4H_6NiO_4{\cdot}4H_2O$ (99.0%), $C_4H_6MgO_4{\cdot}4H_2O$ (99.0%), $C_4H_6CoO_4{\cdot}4H_2O$ (99.5%), and $C_4H_6MnO_4{\cdot}4H_2O$ (99.0%) were dissolved in deionized water with appropriate amounts of acrylic acid and nitric acid, to obtain a transparent solution by quick stirring. The above-mentioned solution was placed in an air blowing thermostatic oven and heating at 180 ℃ for 6h to realize thermal polymerization, thus obtaining a yellowish-brown precursor. The precursor was pre-annealed at 500 ℃, followed by 12h at 950 ℃ in air with a heating rate of 5 ℃/min, finally cooled to room temperature.

Material Characterizations. The crystallization of as-synthesized material was confirmed by X-ray diffraction (XRD), which was carried out on a Bruker D8 Advance Diffractometer (Rigaku D/max-2500) equipped with Cu Kα radiation source (λ = 1.5418 Å) at room temperature. The specific lattice parameters were refined by Fullproof Suite software based on the Rietveld method. The morphological and structural peculiarities as well as atomic images were collected by scanning electron microscopy (SEM, JEOL SU-8020, 10 kV), and transmission electron microscopy (TEM, JEM 2100F, 200 kV). The chemical composition was identified by inductively coupled plasma-mass spectrometry (ICP-MS). *In situ* XRD was collected between 2θ = 10° and 70° at 0.1C upon charging and discharging process by using a special Swagelok cell with an ultra-thin aluminum window for X-ray window for penetration. Meanwhile, *in situ* high-energy XRD (*In situ* HE-XRD) at different temperatures was conducted by Empyrean (PANalytical B.V., Holland) diffractometer.

Electrochemical tests. The working electrodes were prepared by mixing active materials (70 wt%), super P carbon (20 wt%) and poly(vinyl difluoride) binder

(10 wt%) on aluminium foil. The prepared electrodes were dried at a vacuum oven at 80℃ for 12 h and then fabricated into CR2032 coin-type cells by using pure sodium foil as counter electrode, 1 M $NaClO_4$ in (EC: DEC = 1:1, 5vol.% FEC) as electrolyte and porous glass fiber as separator in argon-filled glove box (H_2O, O_2 < 0.1 ppm). The charge and discharge measurements were carried out on a Neware battery test system (CT-4008, Shenzhen, China) under room temperature.

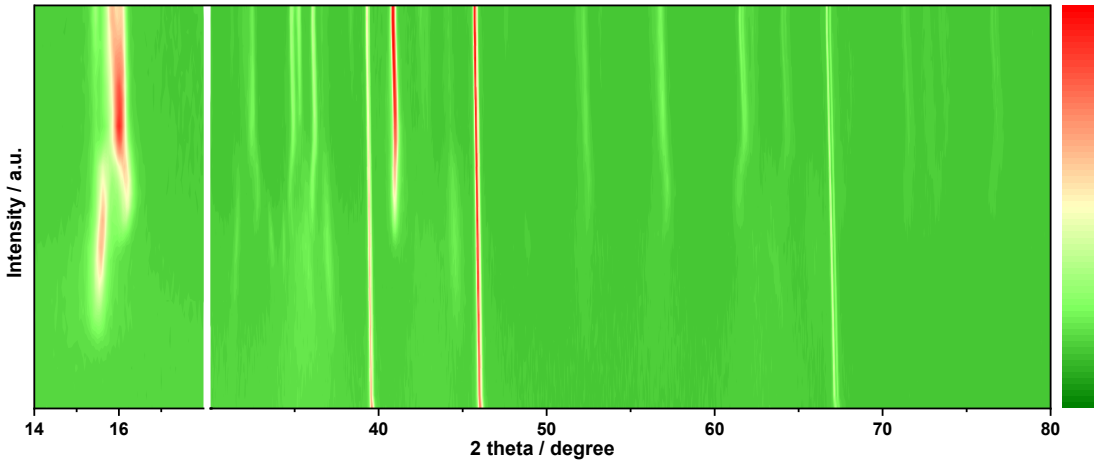

Figure S1. Intensity contour maps of *in situ* high-energy XRD of as-synthesized precursor of P2/P3-NaNCM cathode material during calcination.

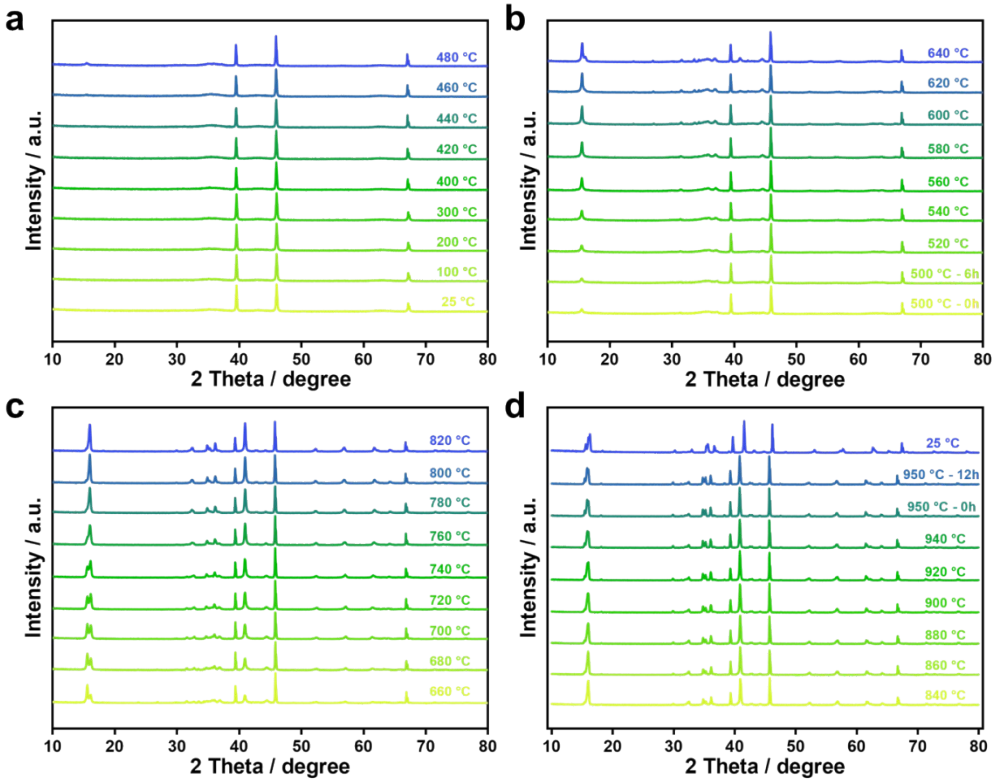

Figure S2. Intensity contour map *in situ* high-energy XRD of as-synthesized precursor of P2/P3-NaNCM cathode material during calcination. (a-d) The detailed calcination and formation process at different temperatures.

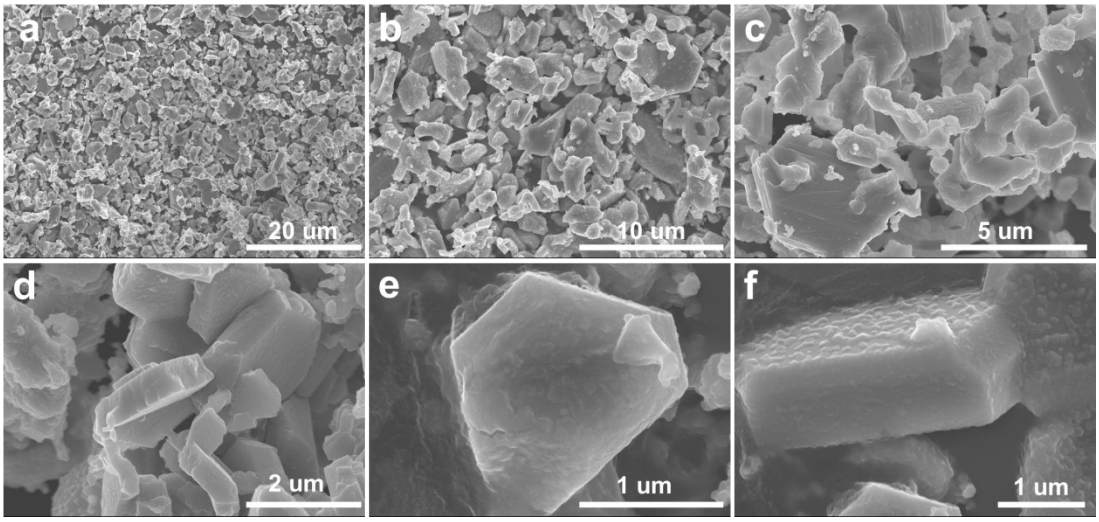

Figure S3. (a-f) SEM images of P2/P3-NaNCM cathode material at different magnification.

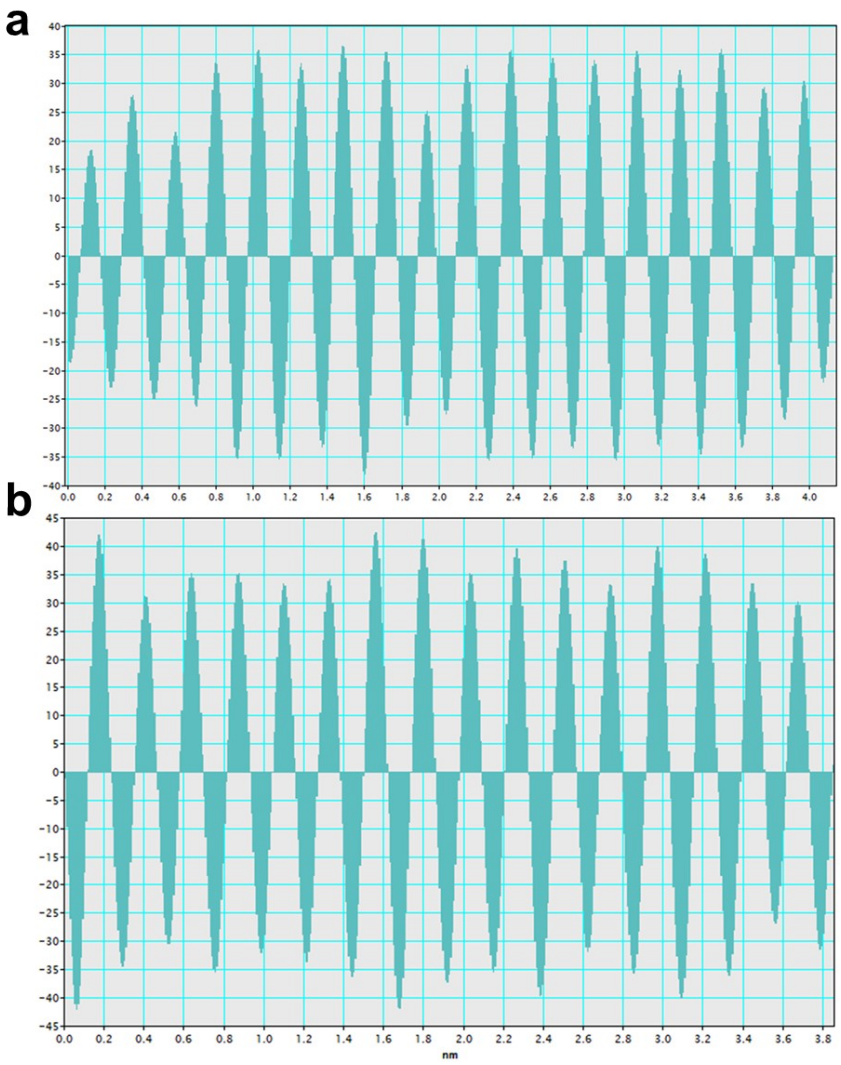

Figure S4. (a, b) Line profiles of P2 phase and P3 phase in P2/P3-NaNCM cathode material.

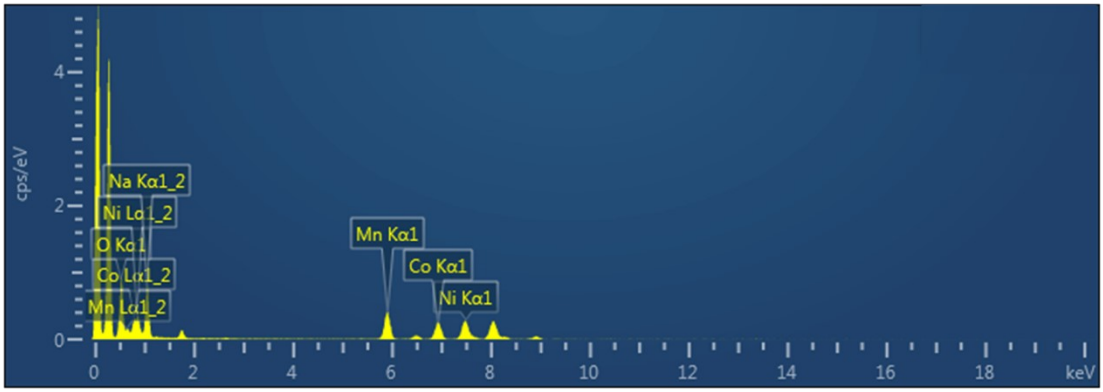

Figure S5. EDS spectrum of P2/P3-NaNCM cathode material.

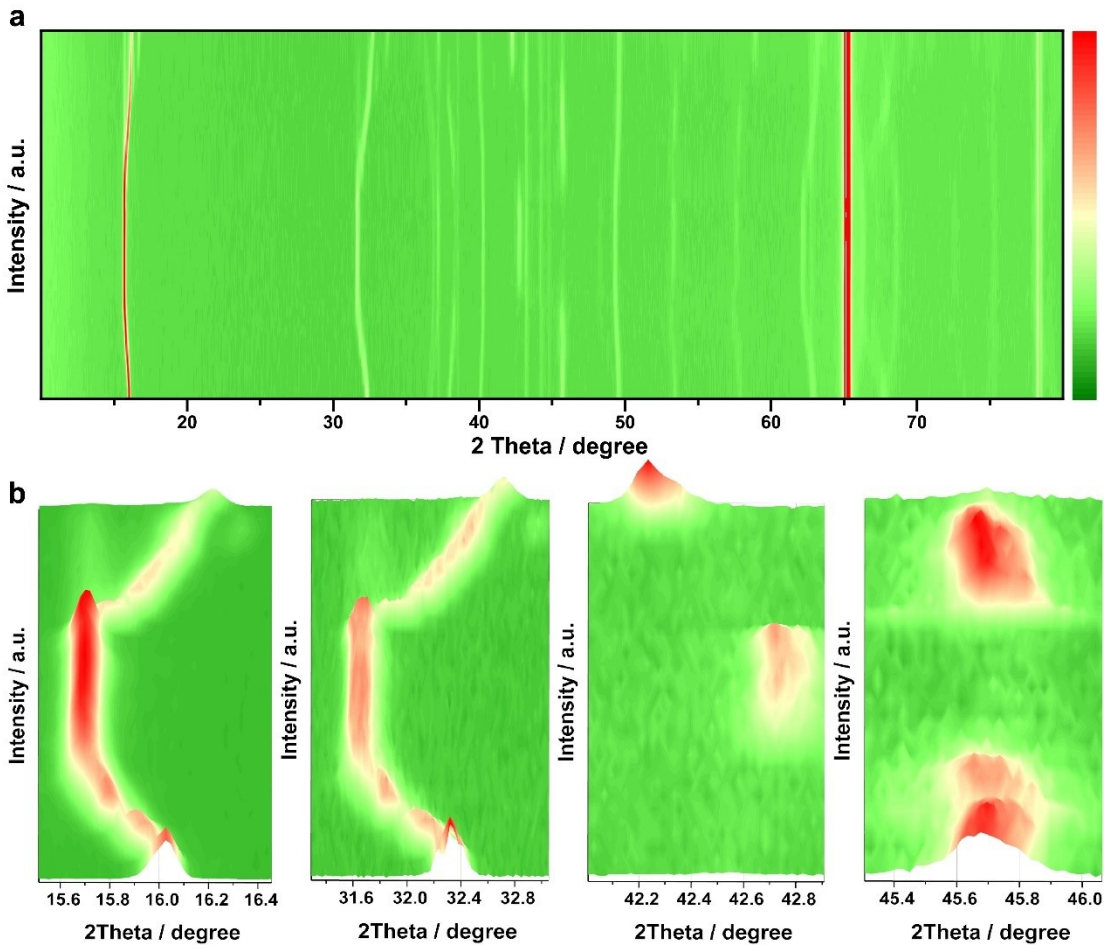

Figure S6. *In situ* charge and discharge XRD of P2/P3-NaNCM cathode material collected during the first cycle at 0.1C. (a) Intensity contour maps and (b) corresponding three-dimensional maps showing the evolution of the main characteristic diffraction peaks.

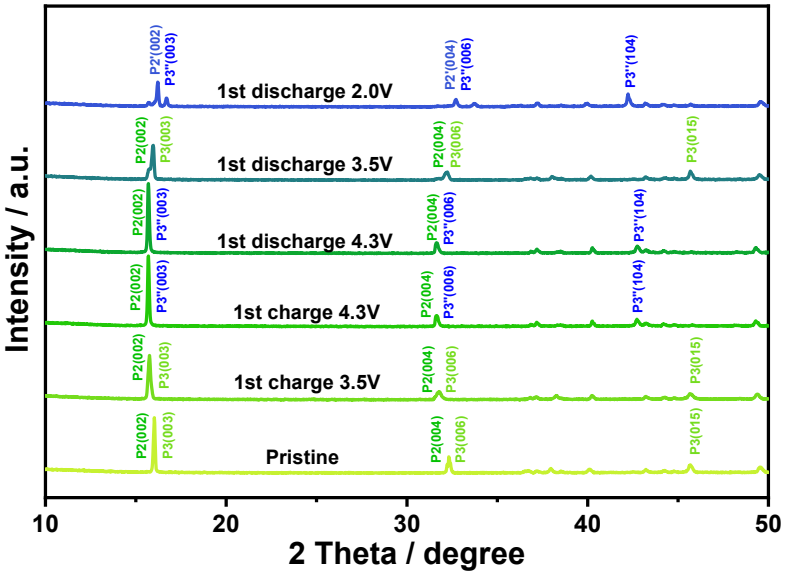

Figure S7. Detailed *in situ* XRD patterns of P2/P3-NaNCM cathode material at different charge and discharge voltages.

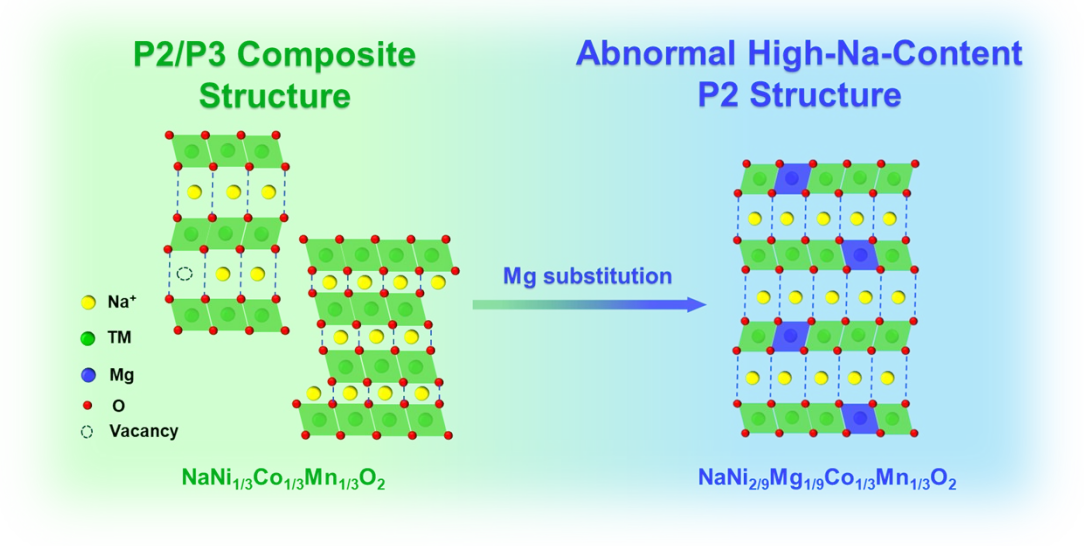

Figure S8. The schematic illustration of structural transformation from a composite P2/P3 structure to a pure P2 structure with high Na content.

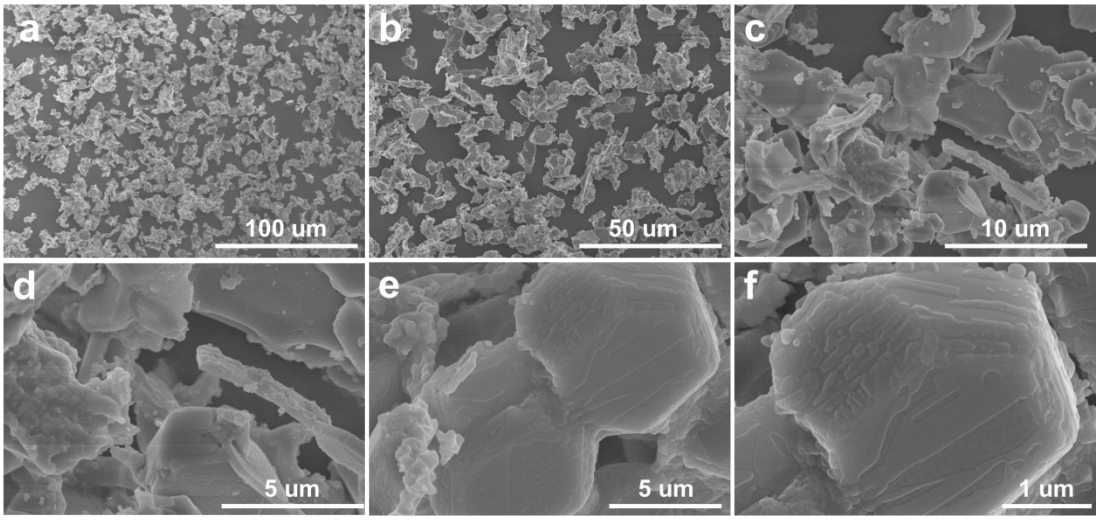

Figure S9. (a-f) SEM images of P2-NaNMCM cathode material at different magnification.

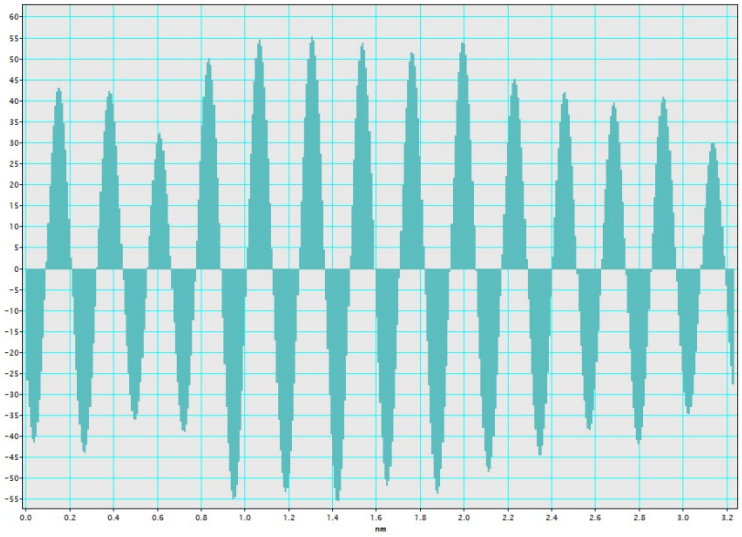

Figure S10. Line profile of P2 phase in P2-NaNMCM cathode material.

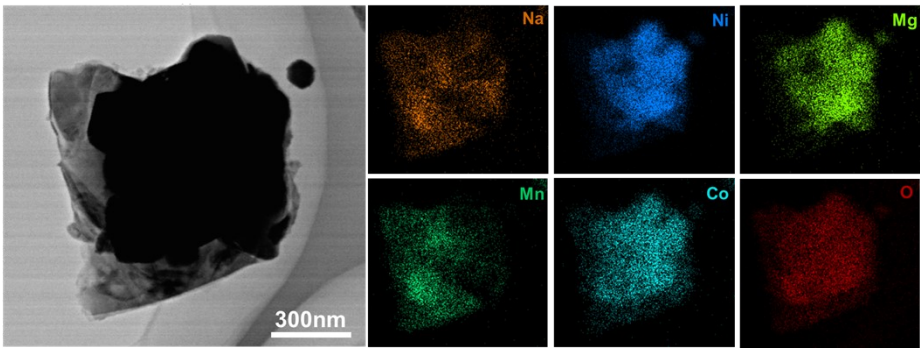

Figure S11. EDS mapping of P2-NaNMCM cathode material.

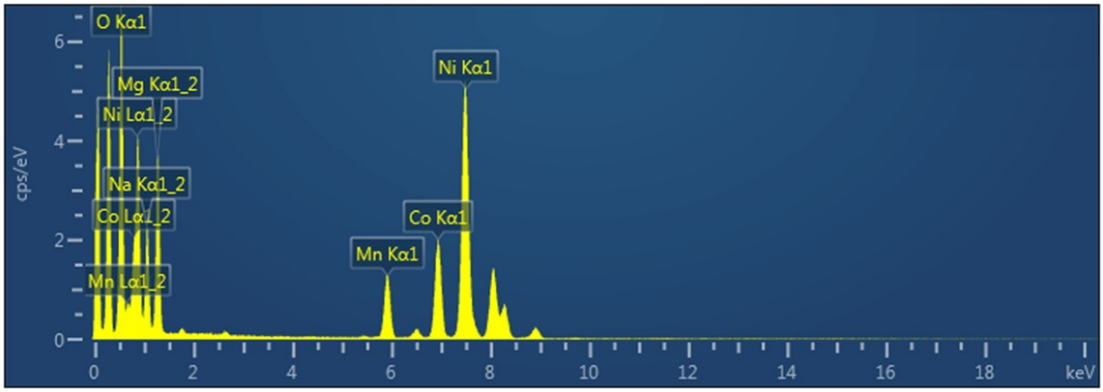

Figure S12. EDS spectrum of P2-NaNMCM cathode material.

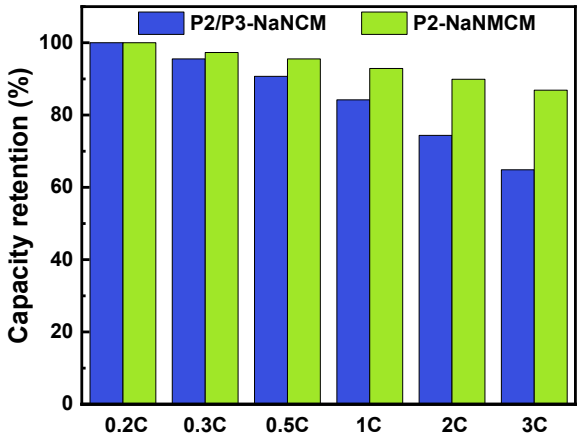

Figure S13. Comparison of capacity retention at different rates corresponding to 0.2C of P2/P3-NaNCM and P2-NaNMCM cathode materials.

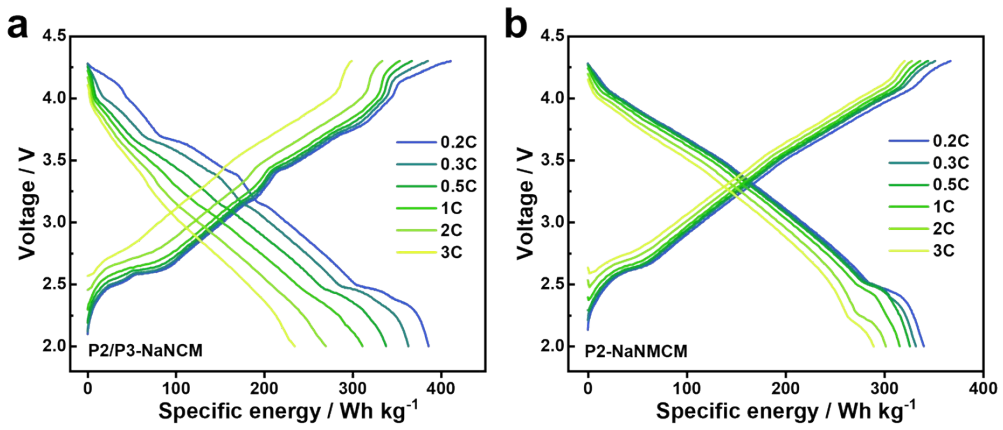

Figure S14. GCD versus specific energy at different rates of (a) P2/P3-NaNCM and (b) P2-NaNMCM cathode materials.

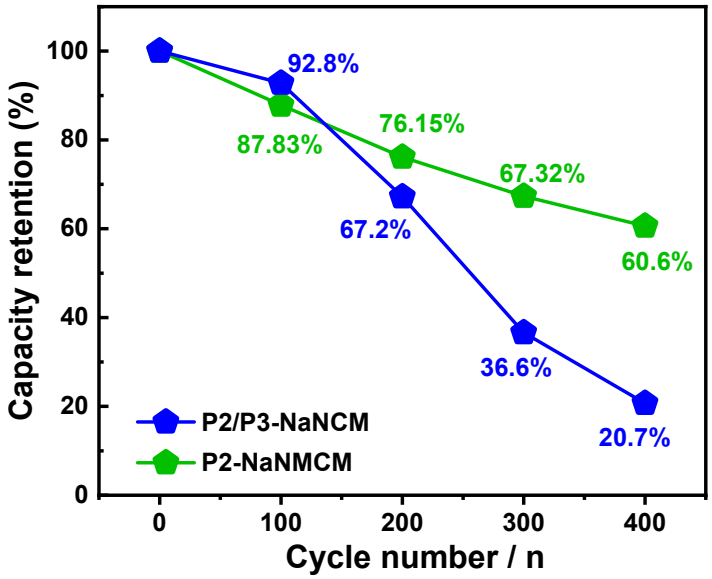

Figure S15. Comparison of capacity retention at different cycles corresponding to the 1st cycle of P2/P3-NaNCM and P2-NaNMCM cathode materials.

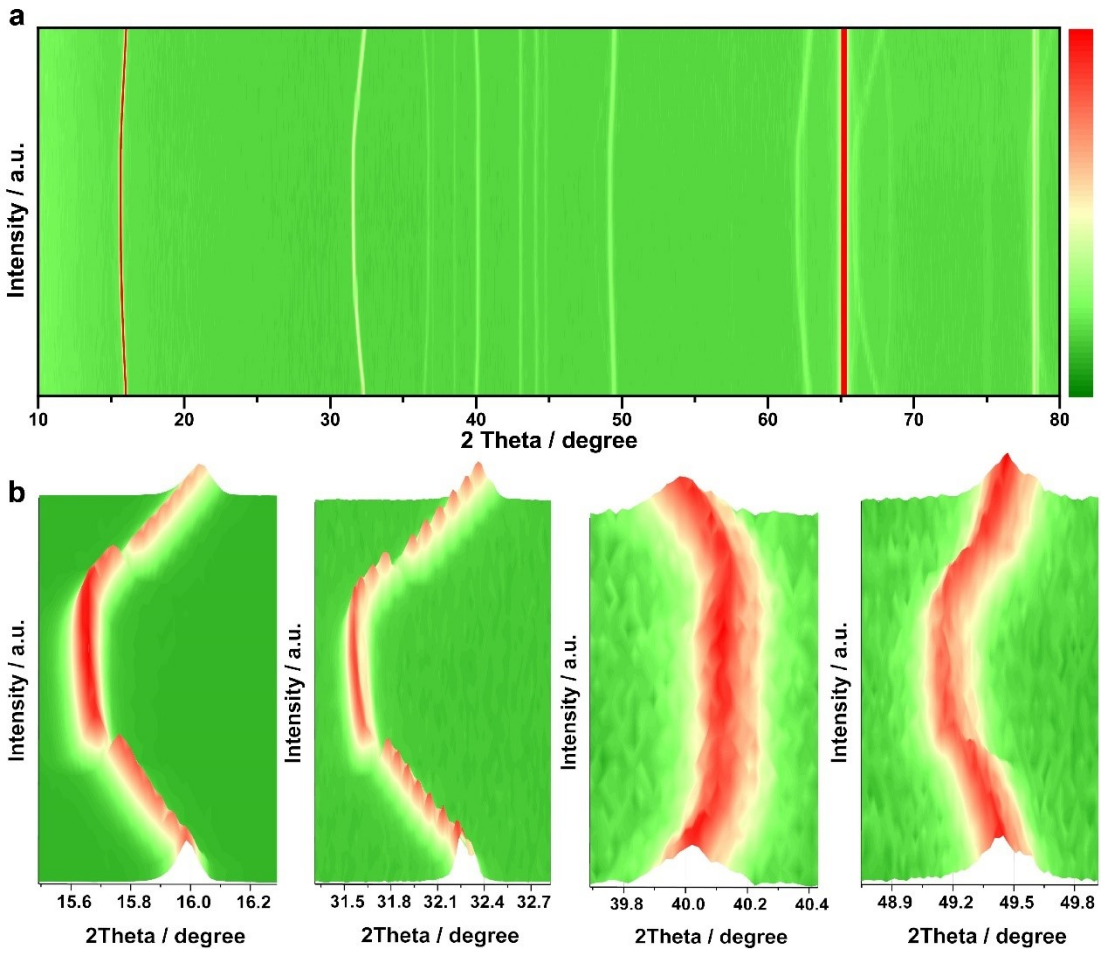

Figure S16. *In situ* charge and discharge XRD of P2-NaNMCM cathode material collected during the first cycle at 0.1C. (a) Intensity contour maps and (b) corresponding three-dimensional maps showing the evolution of the main characteristic diffraction peaks.

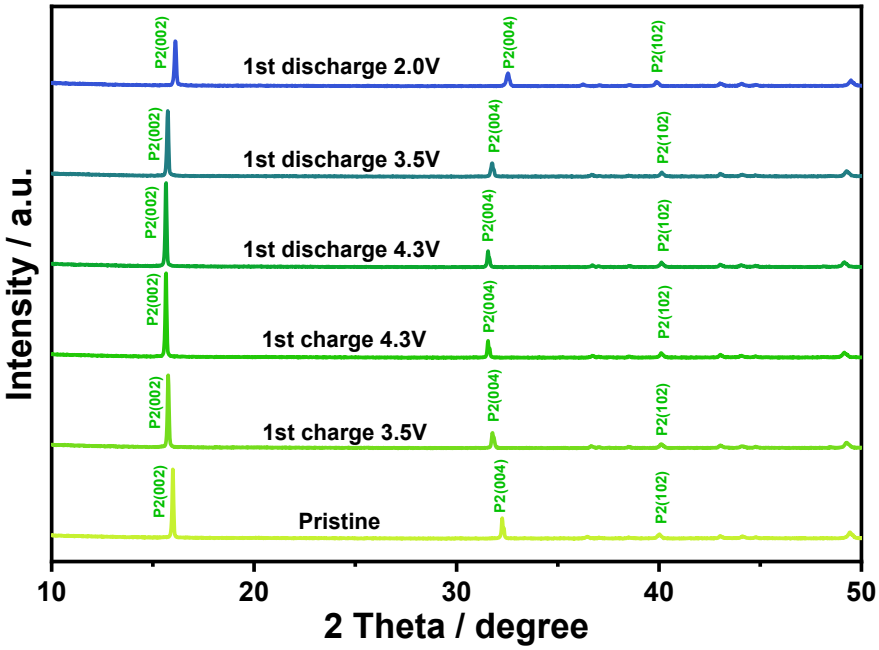

Figure S17. Detailed *in situ* XRD patterns of P2-NaNMCM cathode material at different charge and discharge voltages.

Table S1. Structural information and lattice parameters of P2/P3-NaNCM cathode material form Rietveld refinement.

Sample	Space group	a/Å	b/Å	c/Å	V/Å^3	Mass ratio/%
P2/P3-NaNCM	*R*3m	2.86821	2.86821	16.51461	117.658	68.37
	*P*6$_3$/mmc	2.84426	2.84426	11.07067	77.561	31.63
	R_p = 5.98 %			**R_{wp} = 10.7%**		

Table S2. The ICP-MS result of P2/P3-NaNCM cathode material.

Theoretical chemical formula	Measured atomic ratio			
	Na	Ni	Co	Mn
$NaNi_{1/3}Co_{1/3}Mn_{1/3}O_2$	0.991	0.342	0.336	0.322

Table S3. Structural information and lattice parameters of P2-NaNMCM cathode material form Rietveld refinement.

Sample	Space group	a/Å	b/Å	c/Å	V/Å^3	Mass ratio/%
P2-NaNMCM	$P6_3/mmc$	2.84674	2.84674	11.09131	77.841	100
	R_p = 5.18 %		**R_{wp} = 9.70 %**			

Table S4. The ICP-MS result of P2-NaMNCM cathode material.

Theoretical chemical formula	Measured atomic ratio				
	Na	Ni	Mg	Co	Mn
$NaNi_{2/9}Mg_{1/9}Co_{1/3}Mn_{1/3}O_2$	0.987	0.210	0.127	0.336	0.327

Table S5. Summary of charge and discharge specific capacity (mA h g^{-1}) at different rates for P2/P3-NaNCM and P2-NaNMCM electrodes in half-cell system.

Electrode	0.2C	0.3C	0.5C	1C	2C	3C
P2/P3-NaNCM	126.2/ 125.1	120.0/ 119.3	114.2/ 114.0	107.6/ 106.2	90.9/ 90.4	80.4/ 80.4
P2-NaNMCM	109.6/ 108.0	105.8/ 105.5	104.3/ 103.4	100.9/ 100.4	97.1/ 97	93.6/ 93.7

Table S6. Summary of charge and discharge specific energy (W h kg^{-1}) at different rates concerning P2/P3-NaNCM and P2-NaNMCM electrodes in half-cell systems.

Electrode	0.2C	0.3C	0.5C	1C	2C	3C
P2/P3-NaNCM	411.0/ 386.1	385.3/ 363.1	367.1/ 337.9	353.3/ 311.2	333.5/ 269.7	299.1/ 234.5
P2-NaNMCM	366.9/ 339.9	351.3/ 331.7	344.2/ 325.8	336.1/ 315.5	327.9/ 301.5	320.4/ 289.01